

Localized geomagnetic field anomalies in an underground gas storage

Zhendong Wang^{a,*}, Bin Chen^a, Jiehao Yuan^a, Fuxi Yang^b, Lu Jia^b, Can Wang^a

^a Institute of Geophysics, China Earthquake Administration, Beijing 100081, China

^b Earthquake Agency of Xinjiang Uygur Autonomous Region, Urumqi 830011, China



ARTICLE INFO

Keywords:

Piezomagnetic effect
Local magnetic field
Middle-scale experiment
Anomaly analysis
Underground gas storage

ABSTRACT

To investigate possible piezomagnetic effects associated with imposed tectonic stresses, repeated measurements of total magnetic field in an array (~120 km × 90 km in extent) were performed across the Hutubi underground gas storage (HUGS). Forty repeated measurement stations were established in the HUGS and its surrounding areas. Proton precession magnetometers with a sensitivity of 0.15 nT @ 1 Hz were used to measure the total magnetic field at each repeated station. We conducted two field measurement surveys, one with a minimum pressure during April 2017 and the other with a maximum pressure during November 2017 in the HUGS. The local magnetic field (LMF) of the HUGS and its surrounding areas was obtained after data processing, which included diurnal variation reduction (DVR), secular variation reduction (SVR) and LMF acquisition. The average of the mean standard deviations (σ) of the geomagnetic DVR values were 0.038 nT and 0.045 nT for the first and second field surveys respectively. The amplitude of the LMF varied between about 10 nT and 90 nT in the local area. Negative anomalies with a maximum amplitude of -2.1 nT was observed over a seven-month period (April 2017–November 2017) during the loading process with a constantly increasing pressure in the HUGS. The wide range of negative LMF anomalies shows a negative correlation with the increasing pressure in the HUGS. This result constitutes powerful field observational evidence for the existence of piezomagnetic effects under middle-scale experimental conditions.

1. Introduction

Tectonomagnetism is often employed to investigate the geomagnetic changes associated with various types of tectonic events that occur within the crust such as earthquakes, volcanic eruptions, and fault activity (Nagata, 1969). However, it is also pertinent to experimental investigations into the geomagnetic effects caused by underground nuclear tests, mine explosions, and water storage and drainage within a reservoir (Davis, 1983; Johnston, 1987). Accordingly, many researchers have studied tectonomagnetism and achieved notable success due to its significant application to the prediction of both earthquakes and volcanic eruptions (Zhan, 1989; Gu et al., 2006a).

Observed tectonomagnetic variations can be partially explained by piezomagnetic variations resulting from fluctuations in the magnetic remanence susceptibilities of rocks due to local stress changes (Stacey and Johnston, 1972). Consequently, researchers have conducted many experiments related to the magnetic susceptibility (Wilson, 1922; Kalashnikov and Kapitsa, 1952; Kapicka, 1988, 1990, 1992; Hao et al., 1999; Gilder et al., 2002) and remanent magnetization (Ferre et al., 2014) of rocks in the laboratory. In addition, analytical and numerical modeling endeavors have been employed considerably with the use of

various types of pressure sources, examples of which can be found in (Stacey, 1964; Hao et al., 1982; Okubo and Oshiman, 2004; Currenti et al., 2009; Yamazaki, 2009, 2011a, 2013, 2016; Roskosz et al., 2013; Li and Chen, 2016). Moreover, the U.S.A. (Mueller and Johnston, 1998), China (Zhan et al., 1990), Japan (Nishida et al., 2004, Nishida et al. 2007), Italy (Meloni et al., 1998) and India (Waghmare et al., 2009) have all succeeded in detecting piezomagnetic variations in the field with regard to numerous natural phenomena, including earthquakes, volcanic eruptions and active faults (Johnston and Stacey, 1969; Utada et al., 2000; Negro and Currenti, 2003; Johnston et al., 2006; Currenti et al., 2007; Napoli et al., 2008; Yamazaki, 2011b; Ni et al., 2017). Meanwhile, field investigations and observations of geomagnetic variations associated with reservoirs, nuclear tests and artificial explosions are also related to piezomagnetic effects (Davis and Stacey, 1972; Zhan et al., 1992).

Stress generated changes in susceptibility and remanent magnetization can be easily demonstrated in controlled loading experiments on rock samples in the laboratory. However, there is a huge difference in scale between laboratory loading experiments and natural seismic and aseismic tectonic loading. Therefore, conducting middle-scale field experiments that demonstrate local magnetic anomalies generated by

* Corresponding author at: Institute of Geophysics, China Earthquake Administration, No.5 Minzudaxue Nanlu, Haidian District, Beijing 100081, China.
E-mail address: wangzd0626@sina.cn (Z. Wang).

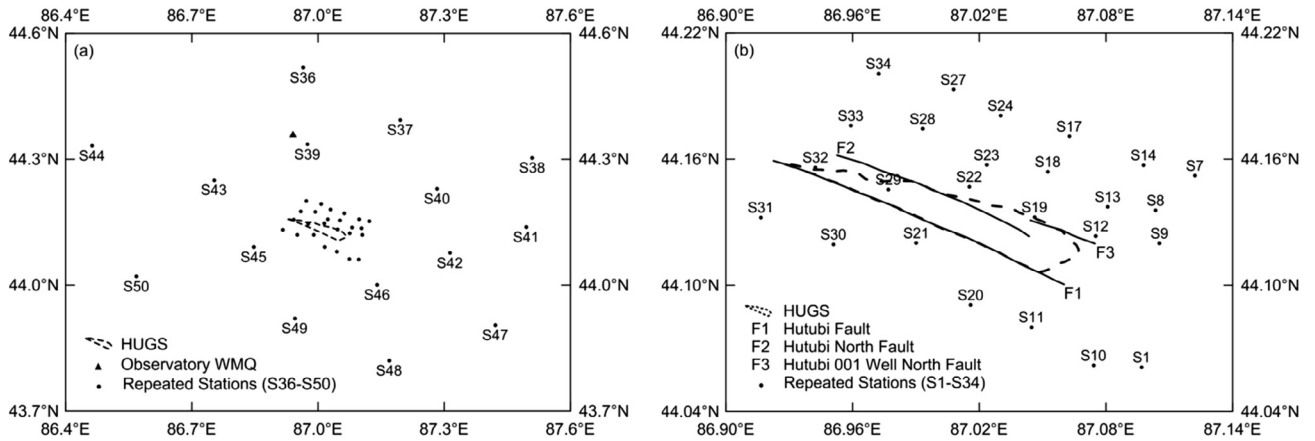


Fig. 1. Map of the research area. Dotted polygon indicates the projected position of the HUGS at the surface. Triangle indicates the location of the continuous geomagnetic observatory WMQ. Solid circles indicate the distribution of repeated geomagnetic stations.

piezomagnetic effects in the Earth's crust is important. The periodic gas injection and extraction process of the large underground gas storage facilities provide large-scale stresses with intensities that are sufficient for producing measurable magnetic anomalies, and thus, they provide an opportunity to observe the effects of piezomagnetism. In this paper, we describe geomagnetic research conducted on the HUGS, which is the largest underground gas storage in China, and we primarily discuss our findings of geomagnetic field anomalies related to imposed tectonic stresses.

2. Field measurements

The acquisition of field data is achieved using a network of forty repeated geomagnetic stations measuring the total magnetic field in the HUGS and its surrounding areas to detect piezomagnetic effects. Fig. 1a shows the distribution of the repeated geomagnetic stations, the location of the continuous geomagnetic observatory WMQ and the HUGS. Three faults in HUGS including the Hutubi Fault (F1), the Hutubi North Fault (F2) and the Hutubi 001 Well North Fault (F3), break through the Ziniqianzi Formation (Fig. 1b). These three fault zones are almost parallel, and they each constitute reverse faults that tend to dip toward the south.

Twenty-five repeated stations are deployed above the HUGS, as indicated by the solid circles in Fig. 1b. The distance between adjacent stations is 2–3 km, and the station code ranges from S1 to S34. In addition, fifteen repeated stations are deployed throughout the peripheral area of the HUGS. The distance between the adjacent peripheral stations is 20–30 km, and the station code ranges from S36 to S50.

Each repeated station is composed of a main sensor post and an auxiliary sensor post with a distance of no less than 20 m between them. To meet the requirements for repeated measurements, both the main sensor post and the auxiliary sensor post are installed with a $15 \times 15 \times 5$ cm non-magnetic acrylic plate as a permanent mark to ensure that the magnetometer sensor remains in the same position. The area around each station has a low magnetic gradient (< 3 nT/m) and manmade electromagnetic interference is absent (Gu et al., 2006b).

3. Data and methods

3.1. Field data

To better observe the dynamic changes in the localized LMF during both gas injection and extraction, the field measurement time is divided into four nodes as follows: 1) the HUGS reaches the gas injection peak with a maximum pressure from the end of October to the beginning of November every year; 2) the HUGS is under continuous gas extraction with a constantly decreasing pressure from the beginning of November

to the end of March of the following year; 3) the HUGS reaches the gas extraction peak with a minimum pressure from the end of March to the beginning of April every year; and 4) the HUGS is subjected to continuous gas injection with a constantly increasing pressure from the beginning of April to the end of October every year.

To acquire the total magnetic field measurements, GSM-19T (GEM Corporation, Canada) proton precession magnetometers (PPM) with a sensitivity of 0.15 nT @ 1 Hz, a resolution of 0.01 nT and an absolute accuracy of ± 0.2 nT were employed. The “exchange synchronous measurement method” was used to calibrate the PPM before and after each measurement to ensure the stability and reliability of the instrument. During the measurement process, PPM was placed on both the main sensor post and the auxiliary sensor post of each station. Three groups were observed simultaneously, and each group recorded ten values of the geomagnetic total intensity. Then, the magnetometers at the main sensor post and auxiliary sensor post were exchanged to repeat the above process. The difference between the main and auxiliary sensor posts and the instrumental difference between the two magnetometers were calculated using the sixty geomagnetic total intensity measurements observed using the synchronous exchange approach. Then, the environmental conditions around each measuring station and the stability of the PPM were analyzed to ensure the accuracy and reliability of the measured data.

3.2. Processing methods

Two total field measurements at all stations were performed with a minimum pressure in the beginning of April 2017 and a maximum pressure in the beginning of November 2017. The data processing scheme includes outdoor data operation and indoor data processing and anomaly analysis (as shown in Fig. 2). The outdoor data operation comprises the preprocessing of the measured data to check for any obvious errors, while the indoor data processing and anomaly analysis are composed of DVR, SVR, LMF acquisition and LMF anomaly analysis (Chen et al., 2017).

3.2.1. DVR

DVR is employed to eliminate regular diurnal variations and other exogenous field components (magnetospheric magnetic field and ionospheric magnetic field) as much as possible in the measured data as follows:

$$\begin{aligned}
 F_{\text{sta_int_}T_i} &= F_{\text{sta_mea_}T_i} - F_{\text{sta_ext_}T_i} \cong F_{\text{sta_mea_}T_i} - F_{\text{obs_ext_}T_i} \\
 &= F_{\text{sta_mea_}T_i} - (F_{\text{obs_mea_}T_i} - F_{\text{obs_int_}T_i}) \cong F_{\text{sta_mea_}T_i} \\
 &\quad - (F_{\text{obs_mea_}T_i} - F_{\text{obs_int_}T_0}) \cong F_{\text{sta_mea_}T_i} - (F_{\text{obs_mea_}T_i} - F_{\text{obs_mea_}T_0})
 \end{aligned} \tag{1}$$

Download English Version:

<https://daneshyari.com/en/article/10121226>

Download Persian Version:

<https://daneshyari.com/article/10121226>

[Daneshyari.com](https://daneshyari.com)